ISSN 1674-1056
http://cpb.iphy.ac.cn
http://iopscience.iop.org/cpb
中国物理 B
Chinese Physics
中国物理 Chinese Physics B

Electronic structures and optical properties of Si-and Sn-doped β-Ga_2O_3: A GGA+*U* study

Jun-Ning Dang(党俊宁), Shu-wen Zheng(郑树文), Lang Chen(陈浪), Tao Zheng(郑涛)
Citation: Chin. Phys. B . 2019, 28(1): 016301. **doi:** 10.1088/1674-1056/28/1/016301
Journal homepage: http://cpb.iphy.ac.cn; http://iopscience.iop.org/cpb

What follows is a list of articles you may be interested in

Ab initio study of H/O trapping and clustering on U/Al interface

Wenhong Ouyang(欧阳文泓), Wensheng Lai(赖文生), Zhengjun Zhang(张政军)
Chin. Phys. B . 2018, 27(9): 097303. **doi:** 10.1088/1674-1056/27/9/097303

Adsorptions of metal adatoms on graphene-like BC_3 and their rich electronic properties: A first-principles study

Pengfei Sui(隋鹏飞), Jiaqi Dai(戴佳琦), Yinchang Zhao(赵银昌), Zhenhong Dai(戴振宏)
Chin. Phys. B . 2018, 27(9): 097311. **doi:** 10.1088/1674-1056/27/9/097311

First-principles study of the $(Cu_xNi_{1-x})_3Sn$ precipitations with different structures in Cu-Ni-Sn alloys

Guang-Wei Peng(彭广威), Xue-Ping Gan(甘雪萍), Zhou Li(李周), Ke-Chao Zhou(周科朝)
Chin. Phys. B . 2018, 27(8): 086302. **doi:** 10.1088/1674-1056/27/8/086302

First principles study of ceramic materials (IVB group carbides) under ultrafast laser irradiation

Nan-Lin He(何南燐), Xin-Lu Cheng(程新路), Hong Zhang(张红), Gai-Qin Yan(闫改琴), Jia Zhang(张佳)
Chin. Phys. B . 2018, 27(3): 036301. **doi:** 10.1088/1674-1056/27/3/036301

Magnetism and piezoelectricity of hexagonal boron nitride with triangular vacancy

Lu-Si Zhao(赵路丝), Chun-Ping Chen(陈春平), Lin-Lin Liu(刘林林), Hong-Xia Yu(于洪侠), Yi Chen(陈怡), Xiao-Chun Wang(王晓春)
Chin. Phys. B . 2018, 27(1): 016301. **doi:** 10.1088/1674-1056/27/1/016301

Electronic structures and optical properties of Si- and Sn-doped β-Ga_2O_3: A GGA+U study*

Jun-Ning Dang(党俊宁), Shu-wen Zheng(郑树文)†, Lang Chen(陈浪), and Tao Zheng(郑涛)

Institute of Opto-electronic Materials and Technology, South China Normal University, Guangzhou 510631, *China*

(Received 17 September2018; revised manuscript received 1 November 2018; published online 25 December 2018)

The electronic structures and optical properties of β-Ga_2O_3 and Si- and Sn-doped β-Ga_2O_3 are studied using the GGA + U method based on density functional theory. The calculated bandgap and Ga 3d-state peak of β-Ga_2O_3 are in good agreement with experimental results. Si- and Sn-doped β-Ga_2O_3 tend to form under O-poor conditions, and the formation energy of Si-doped β-Ga_2O_3 is larger than that of Sn-doped β-Ga_2O_3 because of the large bond length variation between Ga–O and Si–O. Si- and Sn-doped β-Ga_2O_3 have wider optical gaps than β-Ga_2O_3, due to the Burstein–Moss effect and the bandgap renormalization effect. Si-doped β-Ga_2O_3 shows better electron conductivity and a higher optical absorption edge than Sn-doped β-Ga_2O_3, so Si is more suitable as a dopant of n-type β-Ga_2O_3, which can be applied in deep-UV photoelectric devices.

Keywords: density functional theory, GGA + U method, Si-doped β-Ga_2O_3, Sn-doped β-Ga_2O_3, electronic structure, optical property

PACS: 63.20.dk, 73.20.At, 74.20.Pq, 78.20.Ci **DOI:** 10.1088/1674-1056/28/1/016301

1. Introduction

β-Ga_2O_3 is an emerging semiconductor material with a wide bandgap of about 4.9 eV. β-Ga_2O_3 exhibits fascinating physical properties and chemical stability, such as good transparency and a critical breakdown field of up to 8 MV/cm, which has made it a focus of attention in recent years.[1,2] With these advantages, β-Ga_2O_3 is considered to be a promising transparent conducting material operating from the visible to the deep-ultraviolet spectrum for photodetector and other optoelectronic devices.[3,4]

However, the poor electrical conductivity of β-Ga_2O_3 hinders its application as a transparent conducting oxide (TCO).[5] It is well known that doping is an effective way to improve the photoelectric properties of materials, including conductivity, mobility and absorptivity. Si is regarded as a suitable dopant for n-type β-Ga_2O_3 because excess free electrons will be generated after doping. Further, the oxides of Si and Ga have a similar melting point, which is beneficial for adjusting the growth temperature and obtaining a high doping concentration. Zhang *et al.*[6] obtained a Si-doped β-Ga_2O_3 film using the pulsed laser deposition (PLD) technique, and the highest doping concentration is 9.1×10^{19} cm^{-3}, but the corresponding conductivity is only 2.0 S·cm^{-1}. The low conductivity is due to the amorphous-like structure of the Si-doped β-Ga_2O_3 and blockage of electronic transmission paths. Takakura *et al.*[7] deposited Si-doped β-Ga_2O_3 film by radio-frequency (RF) magnetron sputtering, and found that the optical gap of the Si-doped β-Ga_2O_3 is wider than that of β-Ga_2O_3. Recently, a homoepitaxial Si-doped Ga_2O_3 film produced by PLD, with a high carrier concentration of 1.74×10^{20} cm^{-3} and ultrahigh conductivity of 732 S/cm, was reported,[8] but its conductivity is still far below that of commercial ITO film or Al-doped ZnO film. Sn is another promising dopant as a donor for improving the conductivity of β-Ga_2O_3 because excess free electrons will be generated when Sn^{4+} substitutes Ga^{3+}. Orita *et al.*[1] deposited n-type Ga_2O_3 film by Sn doping and obtained the best conductivity of 8.2 S·cm^{-1}. Ohira *et al.*[5] prepared Sn-doped β-Ga_2O_3 by the float-zone method, found that Sn was dispersed in β-Ga_2O_3 uniformly, and suggested that Sn be substituted in the Ga site in the β-Ga_2O_3 lattice, but they did not discuss the optical properties of Sn-doped β-Ga_2O_3. Baldini *et al.*[9] grew Si- and Sn-doped homoepitaxial β-Ga_2O_3 films by metal organic vapor phase epitaxy (MOVPE), and the highest electron concentrations of 8×10^{19} cm^{-3} for Si-doped β-Ga_2O_3 and 1×10^{19} cm^{-3} for Sn-doped β-Ga_2O_3 were obtained. The corresponding electron mobilities were 54.37 cm^2/V·s and 32 cm^2/V·s, but the conductivities and optical properties were not analyzed.

First-principles calculations based on density functional theory (DFT) have been extensively used for scientific research, and some material properties have been successfully parsed, such as electronic structures, optics and magnetism. Varley *et al.*[10] found that a stable structure is obtained when Si^{4+} replaces Ga^{3+} in the four-fold coordination according to the calculated total energy of Si-doped Ga_2O_3 by using first principles. Siah *et al.*[11] reported that Sn^{4+} prefers six-

*Project supported by the Science and Technology Program of Guangdong Province, China (Grant No. 2015B010112002) and the Science and Technology Project of Guangzhou City, China (Grant No. 201607010250).

†Corresponding author. E-mail: LED@scnu.edu.cn

© 2019 Chinese Physical Society and IOP Publishing Ltd

fold coordination and tends to substitute the Ga^{3+} octahedral site for Sn-doped β-Ga_2O_3. Zhang *et al.*[12] calculated the electronic structures and optical properties of β-Ga_2O_3 and Sn-doped β-Ga_2O_3 by using the generalized gradient approximation (GGA) exchange–correlation function based on DFT, but the calculated bandgap of β-Ga_2O_3 is only 2.315 eV, which is less than half of the experimental value (4.9 eV[1]). The underestimation of the bandgap is a well-known drawback of the standard DFT calculation due to the lack of precise consideration of the exchange–correlation potential, but it can be corrected by the scissors approximation,[13] hybrid-functional,[14] and GGA + U methods.[15] In order to obtain calculated bandgaps that are close to the experimental data, Li *et al.*[14] calculated the electrical and optical properties of β-Ga_2O_3 and Si-doped β-Ga_2O_3 using the screened hybrid functional HSE06, but the calculated result shows that β-Ga_2O_3 is a direct-bandgap material, which is not consistent with the experimental result.[16] Lately, Dong *et al.* [15] calculated the influences of oxygen vacancies on the structural and optical properties of β-Ga_2O_3 by GGA + U approximation with the Hubbard U parameters of 7.0 eV and 8.5 eV for Ga and O ions, respectively. The calculated bandgap of β-Ga_2O_3 is 4.92 eV, which is in agreement with the experimental value, but the calculated peak of the Ga 3d state is located at about -14.8 eV, which deviates from the experimental result of -17.12 eV,[17] and so the Hubbard U value requires reconsideration. So far, there have been no reports on the electronic structures and optical properties of Si-doped and Sn-doped β-Ga_2O_3 by using GGA/LDA + U methods. There are also very few comparative research reports on the physical properties of Si-doped β-Ga_2O_3 and Sn-doped β-Ga_2O_3. To further understand the differences in the electronic structures and optical properties of Si-doped β-Ga_2O_3 and Sn-doped β-Ga_2O_3, the energy band structures, density of states and optical properties are calculated in this paper using the GGA + U method based on DFT.

2. Model and method

2.1. Structural model

β-Ga_2O_3 has a monoclinic structure and its space group is $C2/m$,[18] β-Ga_2O_3 has double chains of edge-sharing GaO_6 octahedra and a single chain of vertex-sharing GaO_4 tetrahedra along the y axis, which is beneficial to the movement of free electrons.[19] A $1 \times 2 \times 2$ supercell of β-Ga_2O_3 is used as the father model and is shown in Fig. 1(a). The β-Ga_2O_3 supercell is obtained by expanding a unit cell along the y-axis and z-axis directions, so the supercell has 32 Ga atoms and 48 O atoms. It is noted from Fig. 1(b) that the supercell possesses two inequivalent Ga sites: Ga(1) and Ga(2). The Ga(1) atom bonds with the four nearest oxygen atoms to form a tetrahedral coordinated structure, and the Ga(2) atom bonds with the six nearest oxygen atoms to form an octahedral coordinated structure. When a Si or Sn atom substitutes for a Ga atom in the β-Ga_2O_3 supercell, the Si-doped or Sn-doped β-Ga_2O_3 is obtained and marked as β-$Si_{0.0625}Ga_{1.9375}O_3$ or β-$Sn_{0.0625}Ga_{1.9375}O_3$. To ensure the stability of the doped materials, the structural optimization[30] and total energy calculation of the four doped materials with Si replacing Ga(1) or Ga(2) and Sn replacing Ga(1) or Ga(2) are all carefully considered. The total low-energy results show that β-$Si_{0.0625}Ga_{1.9375}O_3$ with Si replacing Ga(1), and β-$Sn_{0.0625}Ga_{1.9375}O_3$ with Sn replacing Ga(2), are more stable, which are consistent with earlier findings.[10,11] Therefore, the two structural models of β-$Si_{0.0625}Ga_{1.9375}O_3$ with Si replacing Ga(1), and β-$Sn_{0.0625}Ga_{1.9375}O_3$ with Sn replacing Ga(2), are adopted in this paper.

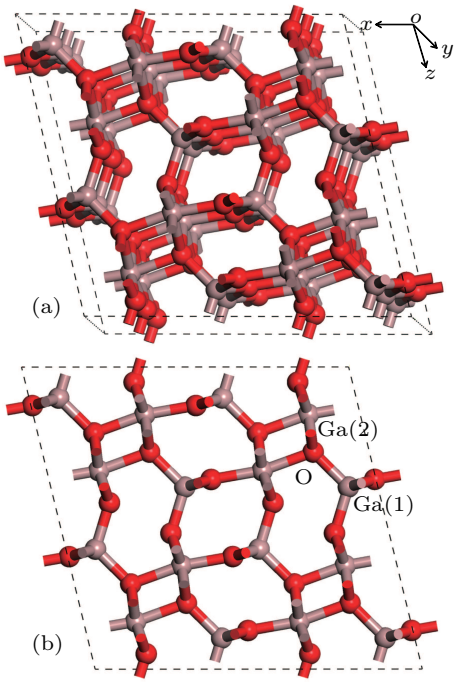


Fig. 1. (a) The $1 \times 2 \times 2$ supercell of β-Ga_2O_3 and (b) the projection along the y-axis direction.

2.2. Computational method

The electronic structures and optical properties of β-Ga_2O_3 and TM-doped β-Ga_2O_3 (TM = Si, Sn) are calculated using the first-principles plane-wave pseudo-potential method based on density functional theory[20] as implemented in the CASTEP package.[21] The exchange–correlation potential is employed through the GGA within the Perdew–Burke–Ernzerhof (PBE) function.[22] The atomic cores are described by the ultra-soft pseudo-potential, and the valence electron configurations are [Ga] $3d^{10}4s^24p^1$, [O] $2s^22p^4$, [Si] $3s^23p^2$ and [Sn] $5s^25p^2$. In order to obtain the accurate bandgap of β-Ga_2O_3, the GGA + U method is adopted and the parameters of $U_{d,Ga}$ and $U_{p,O}$ are set to be 14.0 eV and 8.35 eV, respectively. The energy cutoff of the plane-wave basis is set

to be 450 eV for the calculation of electronic structures and 600 eV for the calculation of optical properties. A $2\times4\times2$ mesh of the Monkhorst–Pack k-points[23] is used for the Brillouin zone integration in reciprocal space.[24] Before calculation, the atomic coordinates and cell volume of the models need to be optimized, and the energy tolerance, tolerance of the force, maximum stress and maximum displacement are set to be 1×10^{-5} eV/atom, 0.03 eV/Å, 0.05 GPa, and 0.001 Å, respectively. The structural optimization is completed when the above four parameters meet or exceed the setting precisions.

3. Results and discussion

3.1. Structural properties

The optimized structure parameters of β-Ga_2O_3 and TM-doped β-Ga_2O_3 (TM = Si, Sn) are listed in Table 1. It is clear that the calculated lattice constants of β-Ga_2O_3 are in good agreement with the experimental results[37] and other calculated data,[38] which indicates that the calculation method and models are rational. The lattice constants of β-$Si_{0.0625}Ga_{1.9375}O_3$ and β-$Sn_{0.0625}Ga_{1.9375}O_3$ are larger than those of β-Ga_2O_3, which mainly originates from the competitive effects of the Coulomb repulsion and the ionic radius difference between Si and Ga or Sn and Ga. On the one hand, the excess free electrons will be generated and will enhance the Coulomb repulsion when Ga^{3+} is replaced by Si^{4+} or Sn^{4+}, and the strong effect of the Coulomb repulsion will increase the supercell volume. On the other hand, the larger ionic radius will increase the volume of the materials. For β-$Si_{0.0625}Ga_{1.9375}O_3$, the Si ionic radius (0.026 nm[27]) is much smaller than that of the Ga(1) (0.047 nm[28]), but the effect of the Coulomb repulsion plays a more important role than the ionic radius difference, so the result of the competition is the supercell volume of β-$Si_{0.0625}Ga_{1.9375}O_3$ being larger than that of β-Ga_2O_3. For β-$Sn_{0.0625}Ga_{1.9375}O_3$, the Sn ionic radius (0.069 nm[29]) is larger than that of the Ga(2) (0.062 nm[28]), and therefore the total superposition makes the supercell volume of β-$Sn_{0.0625}Ga_{1.9375}O_3$ larger than that of β-Ga_2O_3.

Table 1. The structural parameters and formation energies of β-Ga_2O_3 and TM-doped β-Ga_2O_3 (TM = Si, Sn) under the GGA + U method.

		Lattice constant			Volume/Å	E_f/eV	
		a/Å	b/Å	c/Å		O-poor	O-rich
β-Ga_2O_3	this work	12.494	3.092	5.900	221.949		
	Exp.[25]	12.220	3.038	5.786			
	Calc.[26]	12.438	3.084	5.877			
β-$Si_{0.0625}Ga_{1.9375}O_3$		12.516	3.093	5.907	221.998	1.798	4.291
β-$Sn_{0.0625}Ga_{1.9375}O_3$		12.561	3.111	5.926	225.007	1.120	3.615

3.2. Doping formation energy

To evaluate the structure stability of TM-doped β-Ga_2O_3 (TM = Si, Sn), the doping formation energies of β-$Si_{0.0625}Ga_{1.9375}O_3$ and β-$Sn_{0.0625}Ga_{1.9375}O_3$ are calculated according to the formula[30]

$$E_f = E_{TM_{0.0625}Ga_{1.9375}O_3} - E_{\beta-Ga_2O_3} - \mu_{TM} - \mu_{Ga}, \quad (1)$$

where $E_{TM_{0.0625}Ga_{1.9375}O_3}$ is the total supercell energy of β-$Si_{0.0625}Ga_{1.9375}O_3$ or β-$Sn_{0.0625}Ga_{1.9375}O_3$, $E_{\beta-Ga_2O_3}$ is the total supercell energy of β-Ga_2O_3, μ_{TM} represents the chemical potential of the Si or Sn atom, and μ_{Ga} is the chemical potential of the Ga atom. The chemical potential is connected with the growth atmosphere of the materials, which further affects the doping formation energies of TM-doped β-Ga_2O_3. Therefore, the doping formation energies of β-$Si_{0.0625}Ga_{1.9375}O_3$ and β-$Sn_{0.0625}Ga_{1.9375}O_3$ are calculated under O-rich and O-poor conditions. To determine the values of μ_{Ga} and μ_{TM}, the formation enthalpies ΔH_f of β-Ga_2O_3, SnO_2, and SiO_2 are considered assuming their formations from the metallic Ga, Sn, semiconductive Si, and gaseous O_2. The chemical potentials of μ_{Ga} and μ_{TM} are calculated using the following relationships:

$$\mu_{GaO} = 2\mu_{Ga} + 3\mu_O = 2\mu_{Ga(bulk)} + \mu_{O_2} + \Delta H_f(Ga_2O_3), \quad (2)$$

$$\mu_{TMO} = \mu_{TM} + 2\mu_O = \mu_{TM(bulk)} + \mu_{O_2} + \Delta H_f(TMO_2), \quad (3)$$

where μ_{GaO} and μ_{TMO} are the energies of β-Ga_2O_3 and TMO_2 in a single molecule, and $\mu_{Ga(bulk)}$, $\mu_{TM(bulk)}$, and μ_{O_2} are the chemical potentials of metallic Ga, Sn, semiconductive Si, and gaseous O_2, respectively. By combining Eqs. (2) and (3), the chemical potentials of Ga and TM are

$$\mu_{Ga} = \mu_{Ga(bulk)},$$
$$\mu_{TM} = \mu_{TM(bulk)} + \Delta H_f(TMO_2) - \frac{2}{3}\Delta H_f(Ga_2O_3) \quad (4)$$

for O-poor conditions, and

$$\mu_{Ga} = \mu_{Ga(bulk)} + \frac{1}{2}\Delta H_f(Ga_2O_3),$$
$$\mu_{TM} = \mu_{TM(bulk)} + \Delta H_f(TMO_2) \quad (5)$$

for O-rich conditions. The calculated formation enthalpy $\Delta H_f(Ga_2O_3)$ for β-Ga_2O_3 is -10.95 eV, which is close to the experimental value of -11.3 eV.[10] The doping formation energies of β-$Si_{0.0625}Ga_{1.9375}O_3$ or β-$Sn_{0.0625}Ga_{1.9375}O_3$ under O-poor and O-rich conditions are calculated using Eqs. (4) and (5), and the calculated values are listed in Table 1. As

can be seen in Table 1, the doping formation energies of β-$Si_{0.0625}Ga_{1.9375}O_3$ or β-$Sn_{0.0625}Ga_{1.9375}O_3$ under O-poor conditions are lower than those under O-rich conditions, which indicates that the TM-doped β-Ga_2O_3 (TM = Si, Sn) tend to form under O-poor conditions. Moreover, the doping formation energy of β-$Si_{0.0625}Ga_{1.9375}O_3$ is larger than that of β-$Sn_{0.0625}Ga_{1.9375}O_3$ whether under O-rich or O-poor conditions, which reveals that the preparation of Si-doped β-Ga_2O_3 requires a higher growth temperature as compared to Sn-doped β-Ga_2O_3. To explain the difference in the doping formation energy between β-$Si0_{.0625}Ga_{1.9375}O_3$ and β-$Sn0_{.0625}Ga_{1.9375}O_3$, the average bond lengths of Ga(1)–O, Si–O, Ga(2)–O, and Sn–O are given in Table 2. It is well known that the bond length variation is related to the deformation and relaxation of the material structure, which is reflected in the formation energy. It is found from Table 2 that the bond length variation between Ga(1)–O and Si–O is significantly larger than that between Ga(2)–O and Sn–O. Larger bond length variation requires more energy, so the doping formation energy of β-$Si_{0.0625}Ga_{1.9375}O_3$ is larger than that of β-$Sn_{0.0625}Ga_{1.9375}O_3$.

Table 2. The average bond lengths of Ga–O, Si–O and Sn–O for TM-doped β-Ga_2O_3 (TM = Si, Sn).

	Ga(1)–O	Si–O	Ga(2)–O	Sn–O
Average/Å	1.875	1.665	2.033	2.129
Variation/%	11.2		4.5	

3.3. Energy band structure and density of states

To illustrate the effect of the Hubbard U on the band structure and density of states, the calculated band structures and densities of states (DOSs) of β-Ga_2O_3 under GGA and GGA + U methods are shown in Fig. 2. The high symmetry points in the Brillouin zone are located at Γ(0,0,0), A(0,0.5,0), H(0,0.5,0.5) and K(0,0,0.5), and the Fermi level

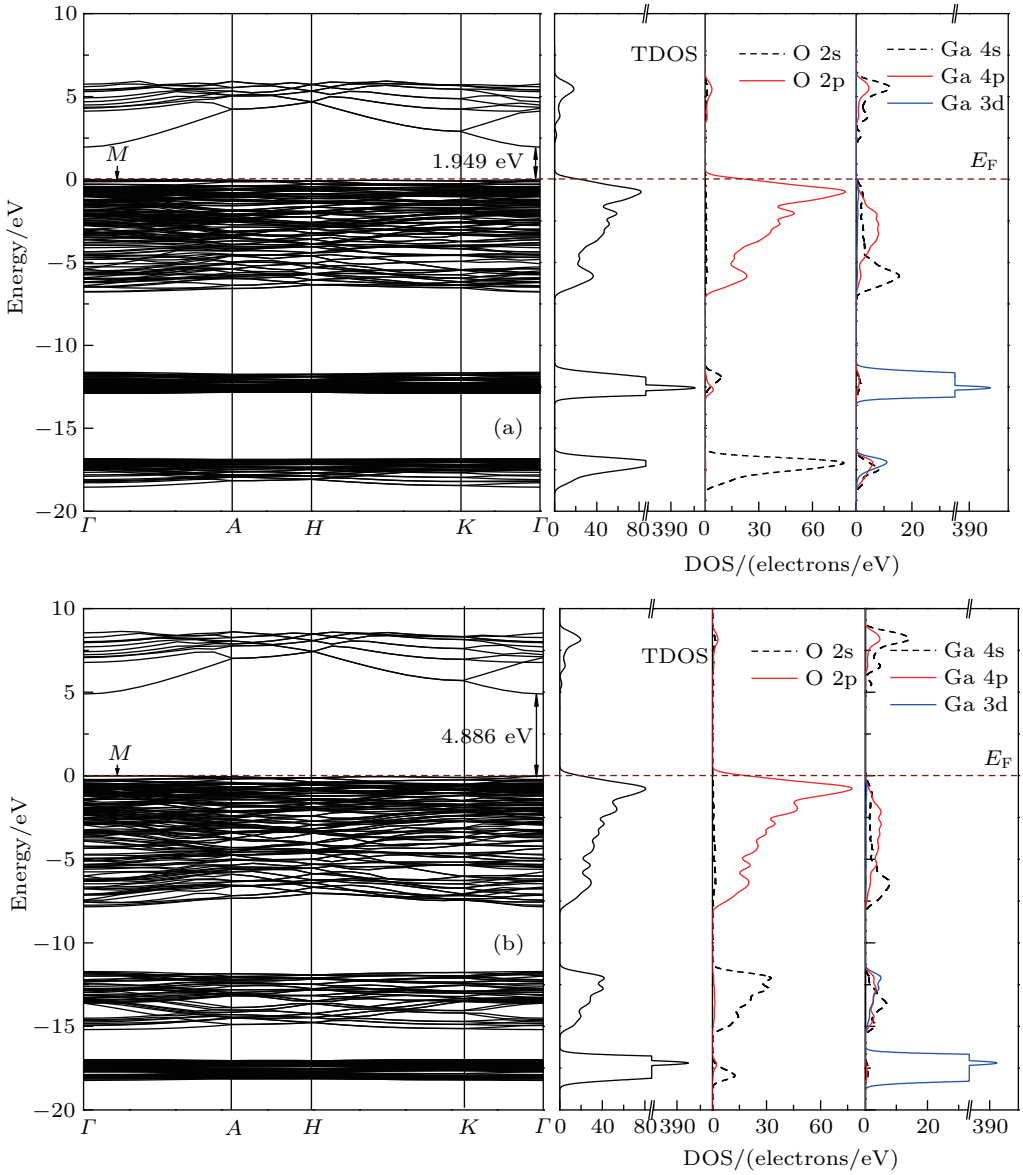


Fig. 2. Band structures and DOSs of β-Ga_2O_3 obtained by (a) GGA and (b) GGA + U methods.

is defined as 0 eV. It can be seen in Fig. 2 that β-Ga_2O_3 has an indirect bandgap with the conduction band minimum (CBM) at Γ point and the valence band maximum (VBM) at M point, which is in agreement with the experimental results.[16] But the direct Γ^+–Γ^- transition is dominant in the optical spectra because the difference between the direct bandgap (Γ^+–Γ^-) and the indirect bandgap (Γ^+–M) is very small (about 0.023 eV), which is proved by the analysis of the dipole transition matrix element and the experimental results of transmission spectra,[31] so the direct Γ^+–Γ^- transition of β-Ga_2O_3 merits more attention than the indirect Γ^+–M transition in optics. As can be seen in Fig. 2(a), the bandgap of β-Ga_2O_3 under the GGA approximation is only 1.949 eV, which deviates significantly from the experimental result of 4.9 eV.[1] Besides, the upper valence bandwidth is only 6.78 eV, which does not agree with the experimental value of about 7.37 eV.[16] More importantly, the Ga 3d state peak is located at 11.63 eV below the VBM, which is not consistent with the experimental result of -17.12 eV.[17] In order to correct the above deviation, the GGA + U method is used and the corrected bandgap of β-Ga_2O_3 is about 4.886 eV (see Fig. 2(b)). At the same time, the upper valence bandwidth is 7.29 eV and the Ga 3d state peak is at -17.01 eV, which are in good agreement with the previous experimental results, so the electronic structures calculated by the GGA + U method are reasonable. Moreover, as can be observed from the partial DOSs in Fig. 2(b), the CBM is dominated by the Ga 4s state and the VBM is occupied by the O 2p state, so the bandgap of β-Ga_2O_3 is determined by O 2p and Ga 4s states, which is consistent with the other calculations.[32]

To further investigate the effect of the doping atom on the electronic structure of β-Ga_2O_3, the band structures and DOSs of β-$Si_{0.0625}Ga_{1.9375}O_3$ and β-$Sn_{0.0625}Ga_{1.9375}O_3$ obtained by the GGA + U method are shown in Fig. 3. The bandgaps E_g of β-$Si_{0.0625}Ga_{1.9375}O_3$ and β-$Sn_{0.0625}Ga_{1.9375}O_3$ are 4.821 eV and 4.613 eV, which are smaller than that of β-Ga_2O_3. But the optical gaps E_g^o (defined as the vertical distance from the Fermi level to the VBM) of β-$Si_{0.0625}Ga_{1.9375}O_3$ and β-$Sn_{0.0625}Ga_{1.9375}O_3$ are 5.853 eV and 5.586 eV, larger than that of β-Ga_2O_3, which is consistent with the experimental result.[7] The electron transition of absorption spectra is related to the optical gap, and the optical gap is an important physical parameter for a TCO material, so β-$Si_{0.0625}Ga_{1.9375}O_3$ has the largest optical gap and is more suitable for application in photoelectric devices as a deep-ultraviolet TCO than are β-Ga_2O_3 and β-$Sn_{0.0625}Ga_{1.9375}O_3$.

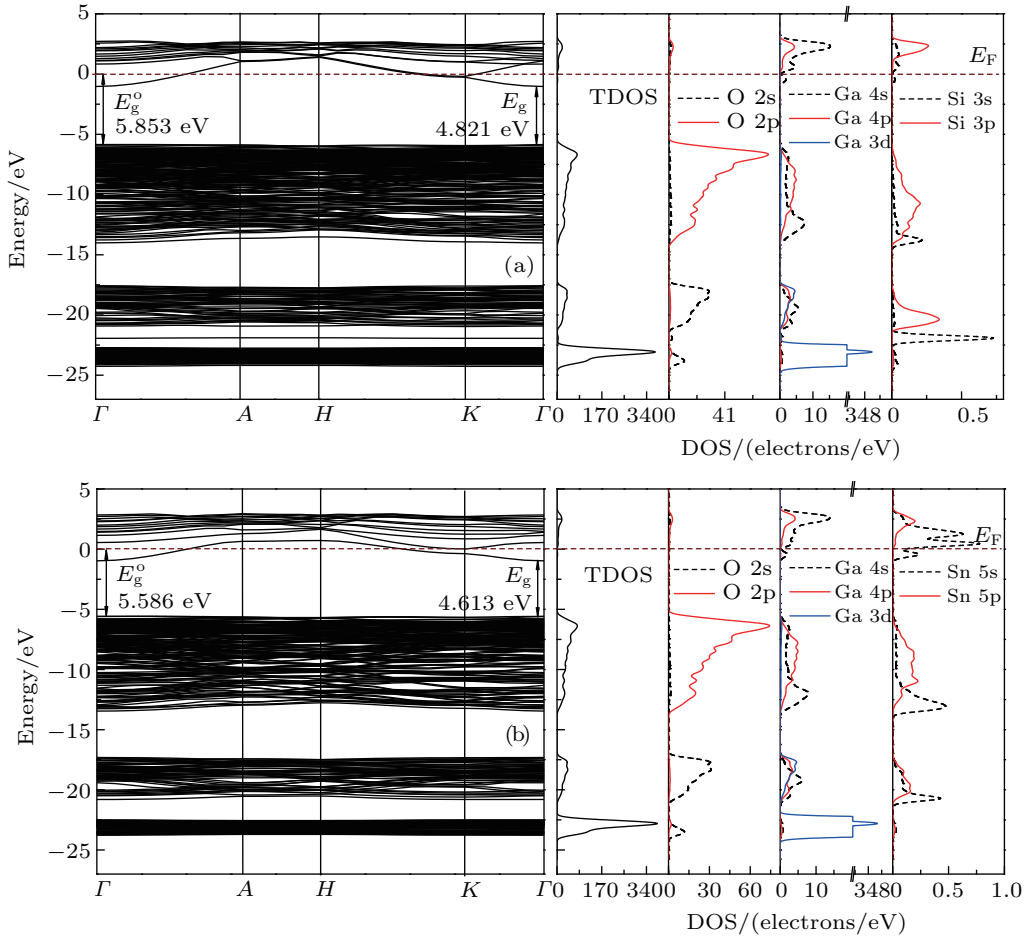


Fig. 3. Band structures and DOSs of (a) β-$Si_{0.0625}Ga_{1.9375}O_3$ and (b) β-$Sn_{0.0625}Ga_{1.9375}O_3$.

The total and the partial densities of states of β-$Si_{0.0625}Ga_{1.9375}O_3$ and β-$Sn_{0.0625}Ga_{1.9375}O_3$ are also given in Fig. 3. For β-$Si_{0.0625}Ga_{1.9375}O_3$, the VBM is occupied by the O 2p state, whereas the CBM is occupied by the Si 3s state, so the bandgap of β-$Si_{0.0625}Ga_{1.9375}O_3$ is determined by O 2p and Si 3s states. It can also be seen in Fig. 3(a) that the DOS of β-$Si_{0.0625}Ga_{1.9375}O_3$ moves along the low energy direction after doping and the Fermi level enters into the conduction band, which indicates the n-type semiconductor feature. Therefore, the conductivity of Si-doped β-Ga_2O_3 is significantly improved compared to that of β-Ga_2O_3, which is consistent with the experiment result.[33] For β-$Sn_{0.0625}Ga_{1.9375}O_3$ in Fig. 4(b), the VBM is occupied by the O 2p state and the CBM is occupied by the Sn 5s state, so the bandgap of β-$Sn_{0.0625}Ga_{1.9375}O_3$ is determined by O 2p and Sn 5s states. Further, the free electrons from Sn 5s state fill the CBM and improve the conductivity of β-$Sn_{0.0625}Ga_{1.9375}O_3$, which is similar to the scenario for β-$Si_{0.0625}Ga_{1.9375}O_3$.

3.4. Electron effective mass and conductivity

For a doped semiconductor with high doping concentration (i.e., $> 10^{19}$ cm^{-3}), there are primarily two competing mechanisms affecting its optical gap: the Burstein–Moss effect[34] and the bandgap renormalization effect.[35] The Burstein–Moss effect causes bandgap widening due to the Fermi-band filling effect, marked as $\Delta E_{\rm BM}$. The bandgap renormalization effect causes bandgap narrowing due to the many-body bandgap renormalization effect and the semiconductor–metal transition effect, labeled as $\Delta E_{\rm BGN}$. The $\Delta E_{\rm BM}$ and $\Delta E_{\rm BGN}$ can be obtained by[36]

$$E_{\rm g}^{\rm o} = E_{\rm go} + \Delta E_{\rm BM} - \Delta E_{\rm BGN}, \tag{6}$$

$$E_{\rm g} = E_{\rm go} - \Delta E_{\rm BGN}, \tag{7}$$

where $E_{\rm go}$ denotes the bandgap of the undoped β-Ga_2O_3, $E_{\rm g}^{\rm o}$ is the optical gap, and $E_{\rm g}$ is the bandgap. According to the band structures in Figs. 2–4, $E_{\rm go}$ is 4.886 eV, and $E_{\rm g}$ is 4.821 eV for β-$Si_{0.0625}Ga_{1.9375}O_3$ and 4.613 eV for β-$Sn_{0.0625}Ga_{1.9375}O_3$. By Eqs. (6) and (7), the $\Delta E_{\rm BM}$ of β-$Si_{0.0625}Ga_{1.9375}O_3$ and β-$Sn_{0.0625}Ga_{1.9375}O_3$ are 1.032 eV and 0.973 eV, and the $\Delta E_{\rm BGN}$ of β-$Si_{0.0625}Ga_{1.9375}O_3$ and β-$Sn_{0.0625}Ga_{1.9375}O_3$ are 0.065 eV and 0.273 eV, respectively. Further, the electron effective mass $m_{\rm e}^*$ is related to $\Delta E_{\rm BM}$ by the following formula:[12]

$$\Delta E_{\rm BM} = \frac{h^2}{8m_{\rm e}^*}\left(\frac{3n_{\rm e}}{\pi}\right)^{2/3}, \tag{8}$$

where h is the Planck constant, and $n_{\rm e}$ is the electron concentration. Using Eq. (8), the electron effective mass of β-$Si_{0.0625}Ga_{1.9375}O_3$ is $0.383m_{\rm e}$ ($m_{\rm e}$ is the electron mass) and $0.402m_{\rm e}$ for β-$Sn_{0.0625}Ga_{1.9375}O_3$. The electron conductivity of the n-type material can be expressed as[37]

$$\sigma = n_{\rm e}qu = \frac{n_{\rm e}q^2\tau}{m_{\rm e}^*} \propto \frac{n_{\rm e}q^2}{m_{\rm e}^*N_{\rm i}}, \tag{9}$$

where q is the electron charge, μ is the electron mobility and τ is the relaxation time which is related to the ionized concentration ($N_{\rm i}$) and thermodynamic temperature. According to Eq. (9), the electron mobility ratio of β-$Si_{0.0625}Ga_{1.9375}O_3$ to β-$Sn_{0.0625}Ga_{1.9375}O_3$ is 1.035, revealing that the electron mobility of β-$Si_{0.0625}Ga_{1.9375}O_3$ is higher than that of β-$Sn_{0.0625}Ga_{1.9375}O_3$, which is consistent with recent experimental results.[9] Further, the electron conductivity ratio of β-$Si_{0.0625}Ga_{1.9375}O_3$ to β-$Sn_{0.0625}Ga_{1.9375}O_3$ is 1.065 from Eq. (9), so Si-doped β-Ga_2O_3 has an advantage over Sn-doped β-Ga_2O_3 in terms of conductivity.

3.5. Optical properties

Optical properties are important for TCO materials and are expressed by the complex dielectric function $\varepsilon(\omega) = \varepsilon_1(\omega) + {\rm i}\varepsilon_2(\omega)$. The imaginary part $\varepsilon_2(\omega)$ of the complex dielectric function is determined by the momentum matrix elements between the occupied and unoccupied wave functions. The real part $\varepsilon_1(\omega)$ can be evaluated from imaginary part $\varepsilon_2(\omega)$ using the Kramers–Kronig relationship, and the absorption coefficient $\alpha(\omega)$ can be calculated according to the complex dielectric function. The above relationships are described by the following formulas:[38]

$$\varepsilon_2(\omega) = \frac{c}{\omega^2}\sum_{\rm V,C}\int_{\rm BZ}\frac{2}{(2\pi)^3}|M_{\rm CV}(k)|^2 \times \delta\left(E_{\rm C}^k - E_{\rm V}^k - \frac{h}{2\pi}\right){\rm d}^3k, \tag{10}$$

$$\varepsilon_1(\omega) = 1 + \frac{2}{\pi}\rho_{\rm o}\int_0^\infty \frac{\omega'\varepsilon_2(\omega')}{\omega'^2 - \omega^2}{\rm d}\omega', \tag{11}$$

$$\alpha(\omega) = \sqrt{2}\left[\sqrt{\varepsilon_1^2(\omega) + \varepsilon_2{}^2(\omega)} - \varepsilon_1(\omega)\right]^{1/2}. \tag{12}$$

Here, $\rho_{\rm o}$ represents the principal value of the integral, subscripts C and V represent the conduction band and valence band states, respectively, BZ means the first Brillouin zone, k is the reciprocal lattice vector, $|M_{\rm CV}(k)|^2$ denotes the momentum matrix element, c is a constant, ω stands for the angular frequency, and $E_{\rm C}^k$ and $E_{\rm V}^k$ represent the intrinsic energy levels. The imaginary part $\varepsilon_2(\omega)$ of the complex dielectric function is the basis for analyzing the optical properties of any materials.

The imaginary parts $\varepsilon_2(\omega)$ of the complex dielectric function of β-Ga_2O_3, β-$Si_{0.0625}Ga_{1.9375}O_3$ and β-$Sn_{0.0625}Ga_{1.9375}O_3$ in the x, y, and z directions are calculated and shown in Fig. 4. For the $\varepsilon_2(\omega)$ of β-Ga_2O_3, three main peaks at 9.286 eV, 10.587 eV, and 9.506 eV appear in the x, y, and z directions; the corresponding peak intensities are 1.42, 1.316, and 2.134, respectively, which indicates that β-Ga_2O_3

has significant anisotropy. For Si- and Sn-doped β-Ga_2O_3, there are no significant changes in the position of the three main peaks in the x, y, and z directions, but in the low-energy range, two small peaks (about 0.9 eV for β-$Sn_{0.0625}Ga_{1.9375}O_3$ and about 1.05 eV for β-$Si_{0.0625}Ga_{1.9375}O_3$) appear. It is well known that the imaginary part $\varepsilon_2(\omega)$ is related to the electron transition between the energy bands, so the peak of $\varepsilon_2(\omega)$ can be explained by the electronic structures. According to the partial DOS in Fig. 3, the main peak of about 10 eV mainly originates from the interband electron transition between the Ga 4s state of the conduction band and the O 2p state of the valence band, but the main peak edges (near to 5 eV) of β-Ga_2O_3, β-$Si_{0.0625}Ga_{1.9375}O_3$ and β-$Sn_{0.0625}Ga_{1.9375}O_3$ are different because their interband electron transitions are different (the electron transitions of Ga 4s and O 2p for β-Ga_2O_3, Si 3s and O 2p for β-$Si_{0.0625}Ga_{1.9375}O_3$, and Sn 5s and O 2p for β-$Sn_{0.0625}Ga_{1.9375}O_3$). The small peak at about 0.9 eV for β-$Sn_{0.0625}Ga_{1.9375}O_3$ is mainly derived from the electron transition between the Sn 5s state and the O 2p state in the conduction band, and the small peak at about 1.05 eV for β-$Si_{0.0625}Ga_{1.9375}O_3$ is mainly derived from the electron transition between the Si 3s state and the O 2p state in the conduction band. The strength difference of the two small peaks is mainly attributed to the different bonding structures: a Si atom bonds with the four closest oxygen atoms but a Sn atom bonds with the six closest oxygen atoms.

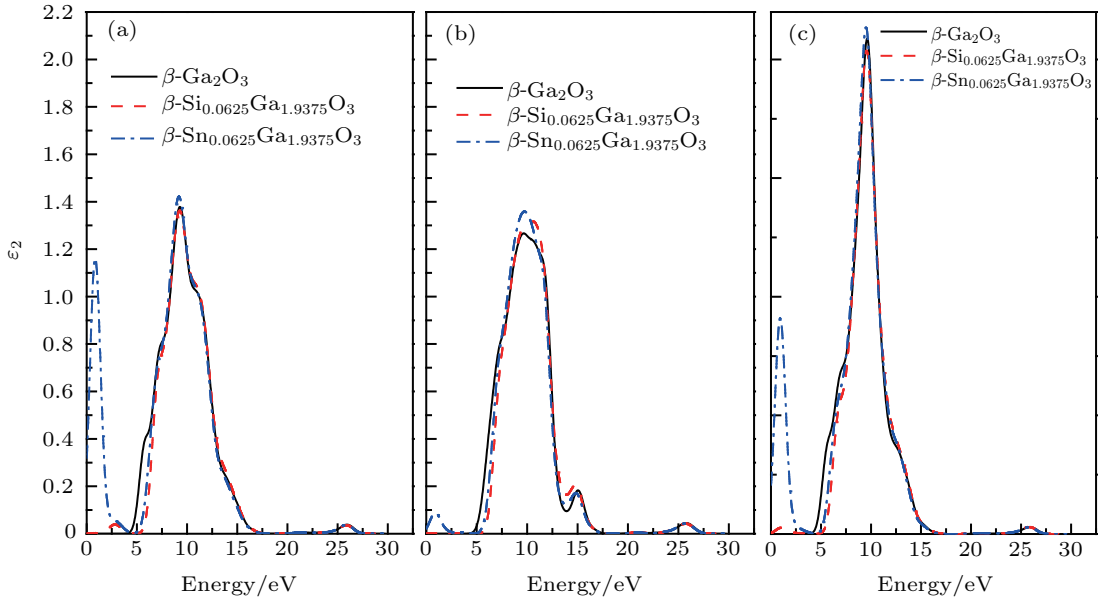


Fig. 4. The imaginary part $\varepsilon_2(\omega)$ of β-Ga_2O_3, β-$Si_{0.0625}Ga_{1.9375}O_3$, and β-$Sn_{0.0625}Ga_{1.9375}O_3$ in the (a) x-axis, (b) y-axis, and (c) z-axis directions.

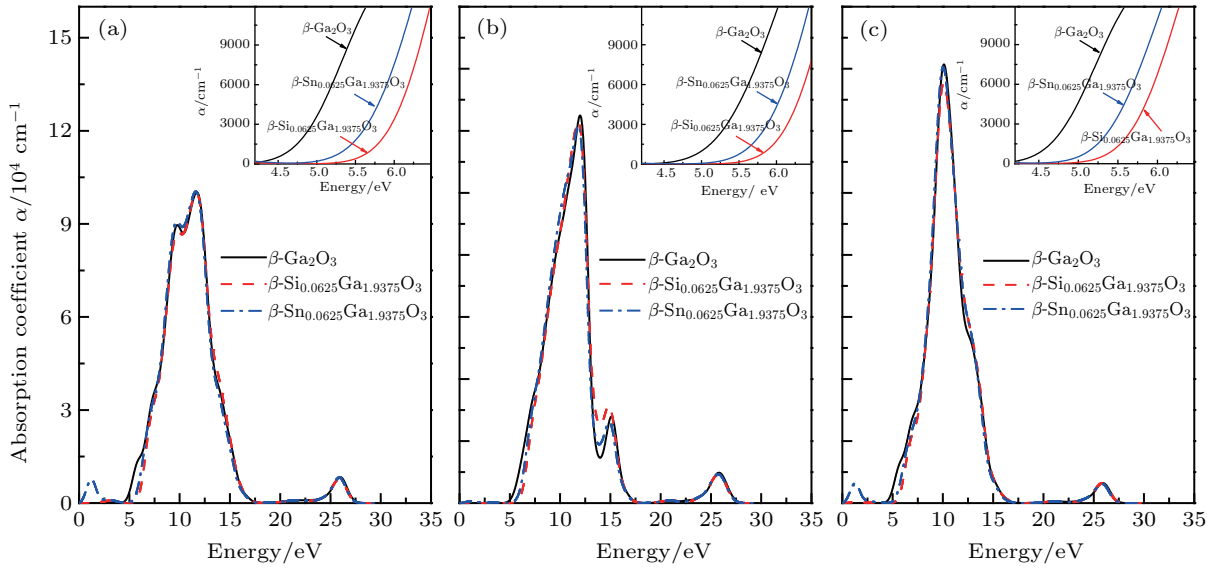


Fig. 5. The absorption coefficients of β-Ga_2O_3, β-$Si_{0.0625}Ga_{1.9375}O_3$ and β-$Sn_{0.0625}Ga_{1.9375}O_3$ in the (a) x-axis, (b) y-axis and (c) z-axis directions. The inset is a partial enlargement.

The absorption coefficients $\alpha(\omega)$ of β-Ga_2O_3, β-$Si_{0.0625}Ga_{1.9375}O_3$ and β-$Sn_{0.0625}Ga_{1.9375}O_3$ in the x, y and z directions are plotted in Fig. 5, and the insets are the partial enlargement. As shown in Fig. 5, the absorption spectra in the x-, y- and z-axis directions are mainly distributed between 5 eV and 17 eV, which are consistent with the imaginary parts $\varepsilon_2(\omega)$ of the complex dielectric function. The main peaks of the absorption spectra along the x-, y- and z-axes are located at 11.6 eV, 12.04 eV and 10.03 eV, respectively, and the peak intensity gradually increases, which is slightly different from the main peaks of the imaginary parts $\varepsilon_2(\omega)$ due to the effect of the real part $\varepsilon_1(\omega)$ of the complex dielectric function. The main peak shapes and intensities are different in the x, y and z directions due to the anisotropy structure, but the peak shapes of β-Ga_2O_3, β-$Si_{0.0625}Ga_{1.9375}O_3$ and β-$Sn_{0.0625}Ga_{1.9375}O_3$ in the same direction are hardly changed except for the edge of the main peak, which means that the main peak is derived from the same electron transition of the Ga 4s and O 2p states and the edge of the peak is related to Si or Sn doping.

To analyze clearly the difference in the peak edge, the spectra between 4.2 eV and 7 eV are also given in the insets of Fig. 5. It can be observed that the optical absorption edges of β-Ga_2O_3 in the x, y, and z directions are 4.753 eV, 5.152 eV and 4.646 eV, respectively, and this explains the cause of the different experimental bandgaps (4.6–5.1 eV) of β-Ga_2O_3 in the literature.[39,40] Moreover, the average optical absorption edge of β-Ga_2O_3 is 4.85 eV, which is very close to the bandgap (4.886 eV) of β-Ga_2O_3 from the band structure in Fig. 2. For β-$Si_{0.0625}Ga_{1.9375}O_3$, the optical absorption edges in the x, y and z directions are 5.897 eV, 6.017 eV and 5.64 eV, respectively, and the average optical absorption edge is 5.851 eV, close to the optical gap of 5.853 eV in Fig. 3. For β-$Sn_{0.0625}Ga_{1.9375}O_3$, the optical absorption edges in the x, y and z directions are 5.592 eV, 5.813 eV and 5.282 eV, respectively, and the average optical absorption edge is 5.562 eV, which is consistent with the optical gap (5.586 eV) of β-$Sn_{0.0625}Ga_{1.9375}O_3$, so the optical absorption edge can be described as a joint band structure between the Fermi level and the VBM. Further, it is noted that the optical absorption edge in the y direction is the largest among the three directions, and the average optical absorption edge of β-$Si_{0.0625}Ga_{1.9375}O_3$ is the largest among them. Figure 5 shows that two small absorption peaks of about 1.2 eV in the x and z directions occur in β-$Sn_{0.0625}Ga_{1.9375}O_3$, but no obvious absorption peaks are found in β-Ga_2O_3 and β-$Si_{0.0625}Ga_{1.9375}O_3$. Therefore, β-$Si_{0.0625}Ga_{1.9375}O_3$ has better light transmittance in the deep-ultraviolet wavelength range than do β-Ga_2O_3 and β-$Sn_{0.0625}Ga_{1.9375}O_3$.

4. Conclusion

In summary, the energy band structures, densities of states and optical properties of β-Ga_2O_3 and β-$TM_{0.0625}Ga_{1.9375}O_3$ (TM = Si, Sn) are calculated and compared using the GGA + U method based on DFT. The calculated bandgap, Ga 3d-state peak and upper valence bandwidth of β-Ga_2O_3 are close to the experimental results if the Hubbard U parameters are set to 14 eV and 8.35 eV for the Ga d state and the O p state. Si- and Sn-doped β-Ga_2O_3 tend to form under O-poor conditions, and Si-doped β-Ga_2O_3 requires higher growth temperature compared with Sn-doped β-Ga_2O_3 because of the large bond length variation between Ga–O and Si–O, but Si-doped β-Ga_2O_3 has better electron mobility and conductivity than Sn-doped β-Ga_2O_3. Besides, the optical properties of Si- and Sn-doped β-Ga_2O_3 show significant anisotropy, and the average optical absorption edge of Si-doped β-Ga_2O_3 is larger than that of β-Ga_2O_3 or β-$Sn_{0.0625}Ga_{1.9375}O_3$, so Si-doped β-Ga_2O_3 has advantages over Sn-doped β-Ga_2O_3 for applications in deep-ultraviolet photoelectric devices.

References

[1] Orita M, Ohta H, Hirano M and Hosono H 2000 *Appl. Phys. Lett.* **77** 4166
[2] Chen K Y C, Hsu C, Yu H C, Peng Y M, Yang C C and Su Y K 2018 *IEEE Trans. Electron. Devices* **65** 1817
[3] Oshima T, Okuno T and Fujita S 2014 *Jpn. Appl. Phys.* **46** 7217
[4] Gaddy B E, Bryan Z, Bryan I, Xie J, Dalmau R, Moody B, Kumagai Y, Nagashima T, Kubota Y and Kinoshita T 2014 *Appl. Phys. Lett.* **104** 202106
[5] Ohira S, Suzuki N, Arai N, Tanaka M, Sugawara T, Nakajima K and Shishido T 2008 *Thin Solid Films* **516** 5763
[6] Zhang F B, Arita M, Wang X, Chen Z W, Saito K, Tanaka T, Nishio M, Motooka T and Guo Q X 2016 *Appl. Phys. Lett.* **109** 102105
[7] Takakura K, Koga D, Ohyama H, Rafi J M, Kayamoto Y, Shibuya M, Yamamoto H and Vanhellemont J 2009 *Physica B* **404** 4854
[8] Leedy K D, Chabak K D, Vasilyev V, Look D C, Boeckl J J, Brown J L, Tetlak S E, Green A J, Moser N A, Crespo A, Thomson D B, Fitch R C, McCandless J P and Jessen G H 2017 *Appl. Phys. Lett.* **111** 012103
[9] Baldini M, Albrecht M, Fiedler A, Irmscher K, Schewski R and Wagner G 2017 *ECS J. Solid State Sci. Technol.* **6** Q3040
[10] Varley J B, Weber J R, Janotti A and Van de Walle C G 2010 *Appl. Phys. Lett.* **97** 142106
[11] Siah S C, Brandt R E, Lim K, Schelhas L T, Jaramillo R, Heinemann M D, Chua D, Wright J, Perkins J D, Segre C U, Gordon R G, Toney M F and Buonassisi T 2015 *Appl. Phys. Lett.* **107** 252103
[12] Zhang Y J, Yan J L, Zhao G and Xie W F 2010 *Physica B* **405** 3899
[13] Zheng S W, Fan G H, He M and Zhang T 2014 *Chin. Phys. B* **23** 066301
[14] Li Y, Yang C H, Wu L Y and Zhang R 2017 *Mod. Phys. Lett. B* **31** 1750172
[15] Dong L P, Jia R X, Xin B, Peng B and Zhang Y M 2017 *Sci. Rep.* **7** 40160
[16] Janowitz C, Scherer V, Mohamed M, Krapf A, Dwelk H, Manzke R, Galazka Z, Uecker R, Irmscher K, Fornari R, Michling M, Schmeisser D, Weber J R, Varley J B and Van de Walle C G 2011 *New J. Phys.* **13** 085014
[17] Wei W, Qin Z X, Fan S F, Li Z W, Shi K, Zhu Q S and Zhang G Y 2012 *Nanoscale Res. Lett.* **7** 1
[18] Ovsyannikov S V and Dubrovinsky L S 2011 *Int. J. High Press. Res.* **31** 23
[19] He H Y, Orlando R, Blanco M A, Pandey R, Amzallag E, Baraille I and Rérat M 2006 *Phys. Rev. B* **74** 195123
[20] Segall M D, Lindan P J D, Probert M J, Pickard C J, Hasnip P J, Clark S J and Payne M C 2002 *J. Phys.: Condens. Matter* **14** 2717

[21] Pallister P J, Moudrakovski I L, Enright G D and Ripmeester J A 2013 *CrystEngComm* **15** 8808
[22] Aspera S M, Sakaue M, Wungu T D K, Alaydrus M, Linh T P T, Kasai H, Nakansishi M and Ishihara T 2012 *J. Phys.: Condens. Matter* **24** 405504
[23] Chen K, Fan G H and Zhang Y 2008 *Acta Phys. Sin.* **57** 1054 (in Chinese)
[24] Fischer T H and Almlof J 1992 *J. Phys. Chem.* **96** 9768
[25] Yoshioka S, Hayashi H, Kuwabara A, Oba F and Matsunaga K 2007 *J. Phys.: Condens. Matter* **19** 1 346211
[26] Kang B K, Mang S R, Go D H and Yoon D H 2013 *Mater. Lett.* **111** 67
[27] Villora E G, Shimamura K, Yoshikawa Y, Ujiie T and Aoki K 2008 *Appl. Phys. Lett.* **92** 202120
[28] Bernd G P, Michel C, Steven G L and Marvin L C 1997 *J. Comput. Phys.* **131** 233
[29] Giacovazzo C, Monaco H L, Viterbo D, Scordari F, Gilli G, Zanotti G and Catti M 1993 *Acta Crystallogr.* **49** 373
[30] Yang K, Dai Y and Huang B 2008 *Chem. Phys. Lett.* **456** 71
[31] Onuma T, Fujioka S, Yamaguchi T, Higashiwaki M, Sasaki K, Masui T, Honda T 2013 *Appl. Phys. Lett.* **103** 041910
[32] Mohamed M, Janowitz C, Unger I, Manzke R, Galazka Z, Uecker R, Fornari R, Weber J R, Varley J B and Van de Walle C G 2010 *Appl. Phys. Lett.* **97** 081906
[33] Sasaki K, Higashiwaki M, Kuramata A, Masui T and Yamakoshi S 2013 *Appl. Phys. Express* **6** 086502
[34] Sarkar A, Ghosh S, Chandhuri S and Pal A K 1991 *Thin Solid Films* **204** 255
[35] Reynolds D C, Look D C and Jogai B 2000 *J. Appl. Phys.* **88** 5760
[36] Zheng S W, Fan G H, Zhang T, Pi H and Xu K F 2014 *Acta Phys. Sin.* **63** 087101
[37] Hou Q Y, Li J J, Ying C, Zhao C W, Zhao E J and Zhang Y 2013 *Chin. Phys. B* **22** 077103
[38] Guo S, Hou Q, Zhao C and Zhang Y 2014 *Chem. Phys. Lett.* **614** 15
[39] Rafique S, Han L and Zhao H P 2015 *Phys. Status Solidi (a)* **213** 1002
[40] Zhang F, Saito K, Tanaka T, Nishio, M and Guo Q 2014 *Solid State Commun.* **186** 28